

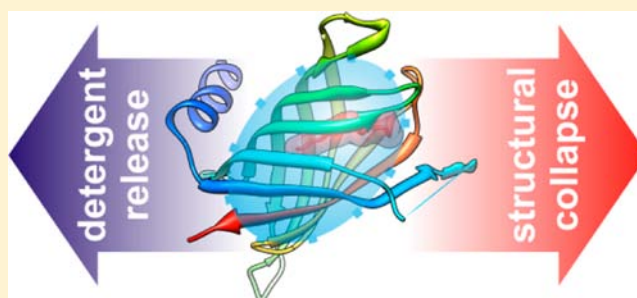
Detergent Release Prolongs the Lifetime of Native-like Membrane Protein Conformations in the Gas-Phase

Antoni J. Borysik, Dominic J. Hewitt, and Carol V. Robinson*

Chemistry Research Laboratory, South Parks Road, University of Oxford, Oxford OX1 3QY, United Kingdom

S Supporting Information

ABSTRACT: Recent studies have suggested that detergents can protect the structure of membrane proteins during their transition from solution to the gas-phase. Here we provide mechanistic insights into this process by interrogating the structures of membrane protein–detergent assemblies in the gas-phase using ion mobility mass spectrometry. We show a clear correlation between the population of native-like protein conformations and the degree of detergent attachment to the protein in the gas-phase. Interrogation of these protein–detergent assemblies, by tandem mass spectrometry, enables us to define the mechanism by which detergents preserve native-like protein conformations in a solvent free environment. We show that the release of detergent is more central to the survival of these conformations than the physical presence of detergent bound to the protein. We propose that detergent release competes with structural collapse for the internal energy of the ion and permits the observation of transient native-like membrane protein conformations that are otherwise lost to structural rearrangement in the gas-phase.



INTRODUCTION

Mass spectrometry (MS) is an exciting new technique for the characterization of membrane proteins and their complexes.^{1–3} Application of MS to the study of membrane proteins is often compromised however by detergents which can remain adsorbed to the protein in the gas-phase resulting in featureless mass spectra. Bound detergent can prove difficult to disrupt even after increasing the ion energy to promote detergent loss by collision induced dissociation (CID). Moreover, this deposition of energy by CID can result in subunit dissociation as well as gas-phase protein unfolding.⁴ Recent studies on the CID of gas-phase detergent clusters, in the absence of protein, have enabled us to identify both charge fission and neutral loss by evaporation as dominant dissociation mechanisms of these clusters.⁵ It also allowed us to propose that detergents could protect gas-phase membrane proteins by a process of “evaporative cooling”.⁶

Here we provide direct evidence that the loss of detergents from a bacterial outer membrane protein (PagP) prolongs the lifetime of native-like conformations of this protein in the gas-phase. Using similar ionization conditions to those commonly used for the gas-phase characterization of soluble proteins, we have generated and maintained a range of different assemblies comprising of PagP and the detergent *n*-dodecyl β -D-maltoside (DDM). Characterization of these assemblies by traveling wave ion mobility mass spectrometry (TWIMS) reveals a clear bimodal character in the arrival time distribution (ATD) of each assembly. The fast ATD component has a collision cross section (Ω) \sim 10% smaller than the native state of PagP and represents conformations that collapse readily on entry to the

solvent-free environment. The slow ATD component has a Ω within a few percent of the Ω of the native protein. Interestingly, the relative population of these ‘native-like’ species increases in line with the degree of DDM attachment to the protein suggesting that the detergent provides protection against gas-phase conformational rearrangement.

To understand the mechanism by which the detergent protects the protein structure from gas-phase collapse, assemblies were interrogated by tandem mass spectrometry (MS/MS) coupled to TWIMS. These experiments show that survival of the native-like conformations is increased for those assemblies that undergo the greatest extent of detergent loss. This allows us to propose that the process of releasing detergent is more central to the survival of the native-like species of PagP than the physical presence of detergent bound to the protein. We suggest that detergent release and gas-phase conformational change are competing pathways for the internal energy of the ion. The release of detergent can therefore provide a “cushion” against conformational collapse and permit the observation of species normally lost to gas-phase rearrangement.

EXPERIMENTAL SECTION

Protein Expression and Purification. Wild-type PagP was expressed with a C-terminal 6His tag in *E. coli* BL21(DE3) cells from the plasmid pETCrcAH Δ S and then resolubilized from inclusion

Received: November 9, 2012

Revised: February 17, 2013

Published: March 25, 2013

bodies into denaturing buffer (6 M Gdn-HCl and 10 mM Tris-HCl pH 8.0) as described previously.⁷ Denatured PagP was purified using a 5 mL His TRAP column (GE Healthcare Life Sciences, Buckinghamshire, U.K.). The protein was eluted with an imidazole gradient and eluted as a single peak above an imidazole concentration of 75 mM. Protein purity was confirmed by SDS-Page electrophoresis of an aliquot of denatured PagP which was first precipitated in water and resuspended in SDS-Page loading buffer. Protein yield was found to be approximately 80 mg/L as confirmed by UV absorbance using a molar extinction coefficient of 82390 M⁻¹ cm⁻¹. Protein samples in denaturing buffer were snap frozen in 1.5 mL aliquots on dry ice and stored at -80 °C.

Protein Refolding and Detergent Exchange. Frozen aliquots of PagP were thawed and refolded using the drop dilution method as described previously.⁷ Briefly 3 mL of denatured PagP solution (approximately 7.5 mg) was slowly diluted dropwise into 40 mL of refolding buffer (0.5% LDAO (*N,N*-dimethyldodecylamine *N*-oxide) 10 mM Tris-HCl pH 8.0) at room temperature with vigorous stirring. The solution was left overnight at 4 °C with gentle agitation and then clarified by centrifugation at 10 000g for 15 min at 4 °C followed by syringe filtration using a 0.45 μm filter to remove any insoluble aggregated material. Refolding of PagP was confirmed by a gel shift assay on NuPAGE Bis-Tris mini gels (Invitrogen, Carlsbad, CA) as previously described.⁷ The folded protein migrated as a single anomalously fast band compared with denatured PagP.

To exchange detergents from 0.5% LDAO to 0.02% *n*-dodecyl-β-D-maltopyranoside (DDM), PagP in refolding buffer was loaded onto a 1 mL His TRAP column equilibrated with 0.1% LDAO and 10 mM Tris-HCl pH 8.0. Bound protein was then washed with a detergent exchange buffer (0.02% DDM and 10 mM Tris-HCl pH 8.0) introduced over a linear gradient. Refolded PagP was then eluted rapidly in 0.02% DDM, 10 mM Tris-HCl pH 8.0, and 200 mM imidazole as a single peak. Protein samples were then snap frozen on dry ice and stored at -80 °C.

Far UV circular dichroism (CD) and an enzyme activity assay confirmed folding of PagP in DDM. An aliquot of frozen PagP was thawed and the imidazole removed by dialysis using 10 kDa MWCO Snakeskin dialysis tubing (Thermo Scientific, Billerica, MA) against 10 mM Tris-HCl pH 8.0. The far UV CD spectrum of the refolded protein in DDM gave a negative ellipticity at 218 nm indicative of a largely β-sheet conformation. Positive ellipticity at 232 nm was also observed in the far UV CD spectrum of refolded PagP due to "cotton effects" anticipated for correct side chain packing of residues lining the lipid binding cleft (Figure S1).⁷ An activity assay monitoring the turnover of the lipid analogue *p*NPP (4-nitrophenyl palmitate, Sigma, U.K.) was performed.⁸ Briefly, 50 μL of 20 mM *p*NPP in isopropanol was added to PagP in 0.02% DDM, 10 mM Tris-HCl pH 8.0 and mixed by rapid inversion. The final protein concentration was 2 μM. The change in absorbance was monitored at 410 nm over 30 min at room temperature. The enzyme turnover rate of *p*NPP by PagP in DDM was found to be ~170 μM min⁻¹ mg⁻¹ and compared well with previously reported values.⁹ The folding of PagP in DDM was also confirmed by a gel shift assay as described above (Figure S1 inset).

Mass Spectrometry. PagP in 0.02% DDM, 10 mM Tris-HCl (pH 8.0) and 200 mM imidazole was thawed and desalted once using a *P*-6 Micro Bio-Spin column (Bio-Rad, Hercules, CA) pre-equilibrated with 200 mM ammonium acetate. The protein was diluted to a concentration of 12 μM in 200 mM ammonium acetate prior to mass spectrometry analysis. The final DDM concentration was estimated to be 0.15 mM. Mass spectra were acquired in positive ion mode on a second generation Synapt HDMS (Waters Corp., Manchester, U.K.) quadrupole-ion trap-IMS instrument fitted with a nanoflow electrospray ionization source (nano-ESI). The instrument was calibrated externally with caesium iodide. Nano-ESI needles were prepared in-house as described previously.¹⁰ Instrumental settings were capillary, cone, trap and transfer voltages of 1.0 kV, 10 V, 10 V, and 5 V, respectively, unless otherwise stated. IMS separation of the ions was performed with a constant wave height of 30 V and a wave velocity of 300 m/s. MSMS was performed at slightly elevated cone voltages (50 V) to promote further dissociation of bound DDM. It

should be noted that the [PagP6DDM]⁶⁺ precursor ion populated a range of different product ions, even under the lower energy conditions used here. Raising the cone voltage served to slightly increase the range of product ions observed.

Ion Mobility Mass Spectrometry. Collision cross sections (Ω) were obtained by traveling wave ion mobility mass spectrometry (TWIMS) as previously described.¹¹ The 7+ to 11+, 14+ to 19+, and 15+ to 21+ ions of ubiquitin (Sigma Aldrich, U6253) cytochrome *c* (Sigma Aldrich, 30396), and horse heart myoglobin (Sigma Aldrich, M1882), respectively, were used as calibrants to enable determination of Ω from experimental drift time measurements. Drift times were obtained for the denatured proteins in 50:50 water-methanol plus 1% acetic acid using the instrumental conditions described above. Drift times for PagP were then obtained without alteration of the IMS wave height, velocity or gas-pressure.

The drift times of the proteins used for calibration were corrected for mass-dependent flight using eq 1, where t'_d is the mass-dependent drift time, t_d the experimental drift time, m/z the mass-to-charge ratio of the ion, and C the instrumental duty cycle.

$$t'_d = t_d - \left[\frac{C\sqrt{m/z}}{1000} \right] \quad (1)$$

The database of Ω for the calibrant ions was corrected for charge and reduced mass using eq 2, where Ω' is the corrected Ω, z the ion charge state, and μ the reduced mass. Ω_{DB} is the database ion Ω in nitrogen.¹² The reciprocal reduced mass of the ion was obtained from eq 3, where m_i and m_g are the ion and gas masses, respectively.

$$\Omega' = \frac{\Omega_{DB}}{z\sqrt{1/\mu}} \quad (2)$$

$$\frac{1}{\mu} = \frac{1}{m_i} + \frac{1}{m_g} \quad (3)$$

An exponential term (X) was obtained from the linear fit of a plot of $\ln t'_d$ against $\ln \Omega'$. This term was used to obtain a corrected ion drift time (t''_d) using eq 4. A plot of t''_d against Ω_{DB} was then used as a calibration plot to obtain the Ω of the drift times recorded experimentally for PagP.

$$t''_d = t'_d \left[\frac{z}{\sqrt{\mu}} \right]^X \quad (4)$$

The R^2 values obtained from the linear fits to the plots of $\ln t'_d$ against $\ln \Omega'$ and t'_d against Ω_{DB} were 0.987 and 0.999, respectively, and were therefore well within anticipated values (Figure S2).¹¹ The Ω for all of the PagP:*n*DDM assemblies did not change significantly (±2%) when determined from ATDs obtained using different IMS wave heights, wave velocities, and gas pressure, recalibrated for these new conditions. The Ω error reported represents the standard deviation of the experimental Ω derived from three independent calibrations. All contour plots were produced using SigmaPlot V 10 (Systat Software, San Jose, CA) using a filled contour plot graph style. The ATDs for each assembly were extracted and converted to Ω using the calibration procedure above.

Modeling of PagP Missing Residues. The N-terminal 7 residues and the C-terminal His-tag missing from the crystal structure of PagP (PDB entry 1THQ) were built onto the structure using Deepview.¹³ Reconstruction of the 10 residues missing in the AB loop was performed using Rosetta which uses a Monte Carlo approach to assemble missing loops using a database of amino acid fragments followed by simulated annealing.¹⁴ Rosetta was used to generate 1000 different models and the model with the lowest all atom score (-670.19) was selected and further energy minimized using CHARM22.¹⁵ The RMSD between the crystal structure (1THQ) and the model generated was 0.19 Å over 146 atom pairs. The Ω of PagP represents the scaled projection approximation (PA) value (PA × 1.14) for the modeled structure that was obtained using drift scope. From this procedure, the calculated Ω of PagP was 22.9 nm².

Circular Dichroism. Far-UV circular dichroism (CD) of PagP was performed on a Chirascan CD spectrometer at 20 °C. The concentration of PagP was 5 μ M, and the concentration of DDM 0.02%. No obvious change was observed in the CD spectrum of PagP on dilution of DDM down to a concentration of 0.003%. Spectra were obtained using a 1 nm step size between 260 and 200 nm; these were then averaged over multiple acquisitions. A blank spectrum was subtracted from the spectrum of PagP, and the ellipticity normalized to the mean residue ellipticity.

Collision Cross Sections of DDM Clusters. Clusters of DDM were obtained using a modified Synapt G1 HDMS mass spectrometer (Waters Corp, Manchester, U.K.) as described previously.⁶ The clusters were obtained in water at a DDM concentration of 5 mM. All reported Ω represent the mean of at least three separate acquisitions. Ω were obtained at a single IMS voltage of 100 V in N_2 , and the data fitted to a standard model of isotropic cluster growth as described previously (Figure S3).⁶

Characterization of Post-IMS Detergent Loss. Mass spectra of PagP were obtained as described above. Interactions between PagP and detergent were disrupted by increasing the collision energy in the transfer region post-IMS. The ATD of the [PagP:0DDM]⁶⁺ ion was extracted over a range of transfer collision energies and converted to Ω .

RESULTS AND DISCUSSION

PagP was expressed and purified from inclusion bodies as previously described.⁷ The protein was refolded into lauryldimethylamine-*N*-oxide (LDAO) and gel-shift analysis. Far UV circular dichroism and turnover of the lipid analogue 4-nitrophenyl palmitate (*p*NPP) confirmed the protein was in the correctly folded state (Figure S1). Mass spectra of PagP in the detergent DDM were obtained on a second generation Synapt HDMS. To minimize conformational rearrangement of PagP in the gas-phase, “gentle” conditions were employed similar to those used for the characterization of soluble proteins.¹⁰ Under these conditions the mass spectrum of PagP spans the 8+ to 5+ charge states. Detergent adducts are also clearly observed (up to +7DDM) for the 7+ to 5+ ions of PagP (Figure 1a). The 6+ and 5+ charge states also contained additional peaks with masses equivalent to the addition of a single LDAO molecule bound to each PagP:*n*DDM assembly.

The gas-phase conformations of the PagP:*n*DDM complexes were investigated by traveling wave ion mobility mass spectrometry (TWIMS).¹⁶ Analysis of the resulting contour plots reveals that the 5+, 6+ and 7+ PagP:*n*DDM assemblies possess bimodal character comprising two distinct populations (Figure 1b). Comparison of the ATDs for each assembly shows that the relative population of each species correlates with the degree of detergent attachment to the protein. For example for the [PagP:0DDM]⁶⁺ assembly the slow ATD component accounts for $\leq 20\%$ of the ion intensity, increasing to $\sim 60\%$ for the [PagP:7DDM]⁶⁺ complex (Figure 1b, inset). A similar trend was also observed for the 5+ and 7+ assemblies (data not shown). The 8+ ions have significantly longer drift times than the other ions in the series, possibly reflecting Coulomb-induced unfolding of PagP or detachment of the C-terminal α -helix from the β -barrel as observed in the solution structure.¹⁷ Other peaks visible in the contour plot originate from “empty” DDM clusters that survive under the gentle instrumental conditions employed. To summarize, PagP:*n*DDM assemblies can be generated and maintained in the gas-phase. Characterization of the assemblies reveals a bimodal character for each complex. The relative population of each species is correlated directly to the degree of detergent attachment with the slow

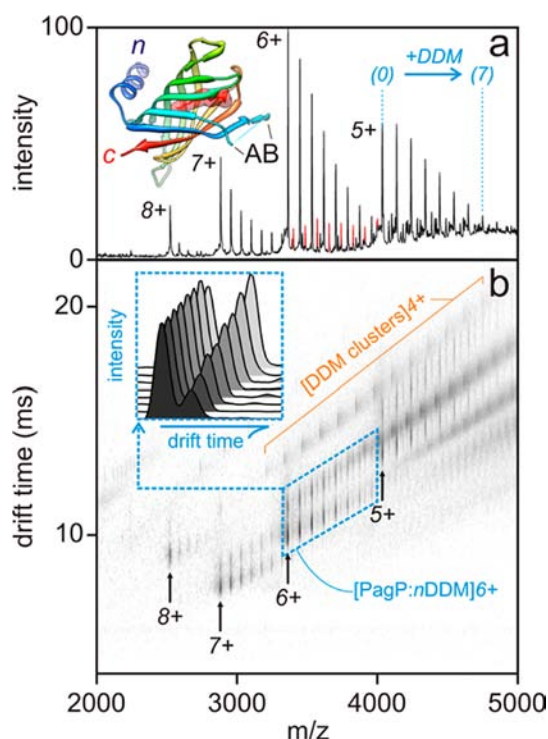


Figure 1. (a) Mass spectrum of PagP in DDM. The 8+ to 5+ ions are labeled and PagP:*n*DDM assemblies are indicated for the 5+ ions with *n*DDM in parentheses. The peaks in the 6+ charge state series (red) are assigned to the LDAO-bound form of PagP. A ribbon representation of the structure of PagP (1THQ) is shown with a space filling representation (red) of the LDAO molecule occupying the lipid-binding cleft of PagP. Residues not present in the X-ray structure are indicated at the N and C-termini as well as in the AB loop. (b) Contour plot associated with (a). DDM-free PagP ions and the charge state are shown (arrows). The ATDs extracted for the [PagP:*n*DDM]⁶⁺ (*n* = 0–7) are shown (inset) with the 0DDM species in the foreground. Other features in the contour plot originate from empty DDM clusters, as indicated for the 4+ DDM cluster charge series. Mass spectra and drift times were obtained on a Waters second generation Synapt HDMS using nitrogen as the buffer gas.

ATD component dominating the ion signal for the species with higher numbers of DDM molecules attached.

To obtain Ω of the PagP:*n*DDM assemblies we calibrated the ion mobility drift times as described above. For the PagP:0DDM assembly the fast ATD component has a Ω of 20.7 ± 0.1 nm² while the slower component has a Ω of 22.1 ± 0.2 nm² (Figure 2). To compare the gas-phase conformations of PagP with the X-ray structure of the protein (1THQ) we used a scaled projection approximation method.^{18,19} The crystal structure of PagP has 23 missing residues, mostly absent from the highly unstructured AB loop of the protein. These were built onto the 1THQ structure using Rosetta.¹⁴ From this procedure, PagP was calculated to have a Ω of 22.9 nm², within 3.5% of the slow component peak but almost 10% larger than the predominant faster, more compact species. This implies that the fast ATD component of PagP represents protein conformations that collapse in the solvent-free environment. Gas-phase protein collapse has been observed previously in soluble proteins containing highly unstructured regions.²⁰

The apparent dependency of the slow ATD component and the presence of bound DDM was then investigated. Activation of the assemblies resulted in an overall disruption of the PagP-*n*DDM interactions (data not shown). The disruption of these

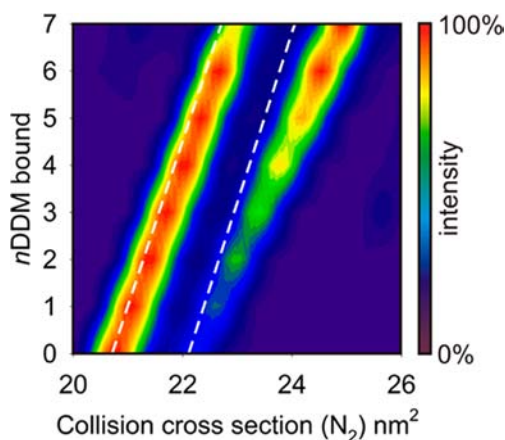


Figure 2. Extracted ATDs converted to Ω for the $[\text{PagP}:n\text{DDM}]^{6+}$ assemblies. Drift times were obtained on a Waters second generation Synapt HDMS in nitrogen. The dashed white lines represent the anticipated changes in Ω with successive addition of DDM for isotropic growth over this size range (Figure S3). The contour plot is a reproduction of the stacked ATDs shown in Figure 1b (inset) and was produced using SigmaPlot V 10 using a filled contour plot function.

interactions coincided with the loss of the slow component in the ATDs of the ions (Figure 3a). To confirm that the slow ATD component was related to a conformation of PagP and not due to post-IMS detergent loss the assemblies were then disrupted in the transfer region (post-IMS) by increasing the transfer collision energy (Figure 3b).

Compared with disruption of assemblies prior to IM, where discrete populations are maintained in the ATDs, disruption in the transfer region results in significantly broadened and diffuse ADTs. This is due to the convergence of many different Ω over a range of $[\text{PagP}:n\text{DDM}]^{6+}$ assemblies. The slow component in the ATDs, perturbed during post IM separation, therefore likely represents a native-like conformation of PagP, the population of which clearly depends on the degree of detergent attachment.

The dependency of Ω on the number of bound DDM molecules ($d\Omega/dn\text{DDM}$) can provide some information on the conformational heterogeneity of the different gas-phase populations of PagP. We found that the $d\Omega/dn\text{DDM}$ for the collapsed protein states of PagP agree closely with the isotropic

changes observed for ‘empty’ DDM clusters over this size range (Figures 2 and S3). This indicates that this collapsed population does not undergo significant conformational changes with increasing numbers of DDM molecules. By contrast the $d\Omega/dn\text{DDM}$ for the native-like populations diverged significantly from anticipated relationships for isotropic growth over this size range. The Ω of the native-like population rises with increasing DDM, consistent with more open conformations with successive DDM attachment. This may reflect different conformational ‘plasticities’ in these ensembles, tense and relaxed forms of PagP have been observed in solution.²¹

The clear correlation between the number of DDM molecules bound to PagP and the population of native-like conformations of this protein implies a simple model by which detergents physically ‘shield’ PagP from conformational collapse. Alternatively, protection of the native-like populations could require bound detergents to be released as neutrals from the assemblies. To differentiate between these alternate models we selected the $[\text{PagP}:6\text{DDM}]^{6+}$ assembly for interrogation by MSMS. The MSMS spectrum of the $[\text{PagP}:6\text{DDM}]^{6+}$ precursor shows that it dissociates readily to form a range of different product ion species $[\text{PagP}:(1-5\text{DDM})]^{6+}$; the precursor ion is also observed in the tandem mass spectrum (Figure 4a). Compact and native-like populations of PagP are observed in the ATDs of these product ions, in line with the observations for the range of $[\text{PagP}:n\text{DDM}]^{6+}$ assemblies present in the mass spectrum. Inspection of the ATDs from the MSMS spectrum shows that increased loss of detergent (from $6n$ to $1n$) is associated with improved survival of the native-like populations of PagP (Figure 4b). If protection of these populations was governed by a shielding mechanism, then the opposite relationship would be expected. This implies therefore that the process of releasing bound detergent is more central to the survival of the native-like populations of PagP than the physical presence of detergent bound to its surface.

We anticipated that the presence of bound LDAO could prevent collapse of the lipid-binding cavity of PagP and help maintain a greater population of the native-like conformation. To test this hypothesis, the ATDs of the LDAO-bound assemblies were obtained (Figure 5a). The results show that the ATDs also possess a bimodal character. Ω of 21.0 and 22.4 nm²

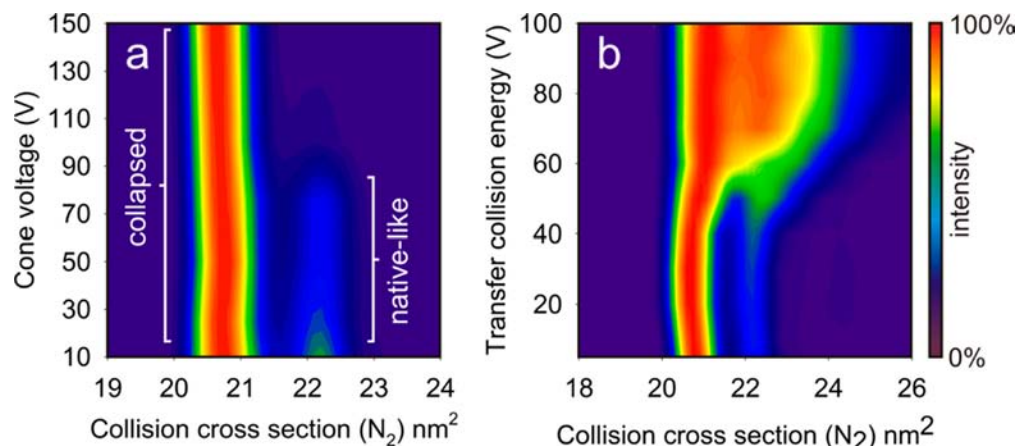


Figure 3. (a) ATDs converted to Ω for the $[\text{PagP}:0\text{DDM}]^{6+}$ assembly as a function of the cone voltage used to promote detergent loss. Collapsed and native-like conformations are indicated. (b) ATDs converted to Ω for the $[\text{PagP}:0\text{DDM}]^{6+}$ assembly as a function of the transfer collision energy used to promote detergent release after ion mobility separation. All drift times were obtained on a Waters second generation Synapt HDMS in nitrogen buffer gas. The contour plots are displayed in Sigma Plot V 10 using a filled contour plot function.

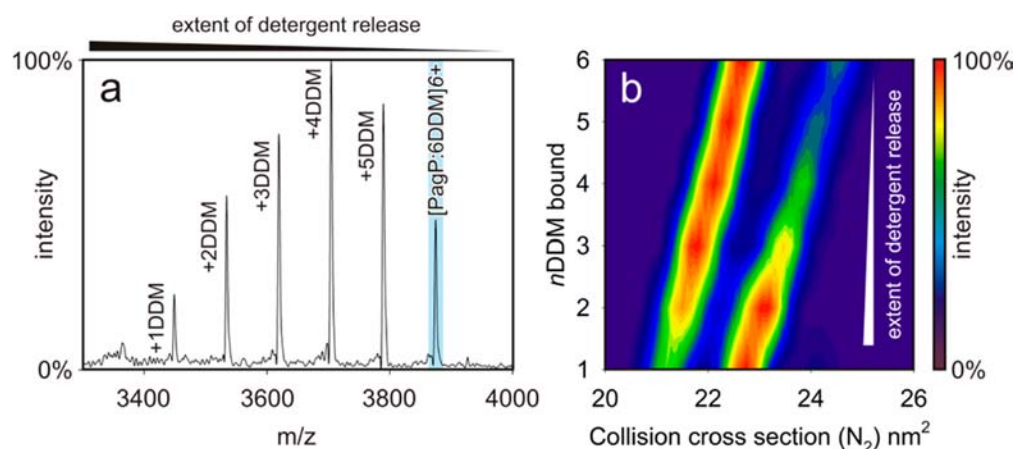


Figure 4. (a) MSMS spectrum of the $[\text{PagP}:6\text{DDM}]^{6+}$ assembly (blue band), five different $\text{PagP}:n\text{DDM}$ products are formed with $n\text{DDM}$ shown. (b) Ω of the $[\text{PagP}:n = 1-5\text{DDM}]^{6+}$ products formed during MSMS of $[\text{PagP}:6\text{DDM}]^{6+}$ the Ω of the precursor ion is also given. All drift times were obtained on a Waters second generation Synapt HDMS in nitrogen buffer gas. Marginal differences in the relative population of the native-like species of the $[\text{PagP}:6\text{DDM}]^{6+}$ assembly observed with either full quadrupole transmission (Figure 2) or MSMS (Figure 4b) are discussed in the Supporting Information.

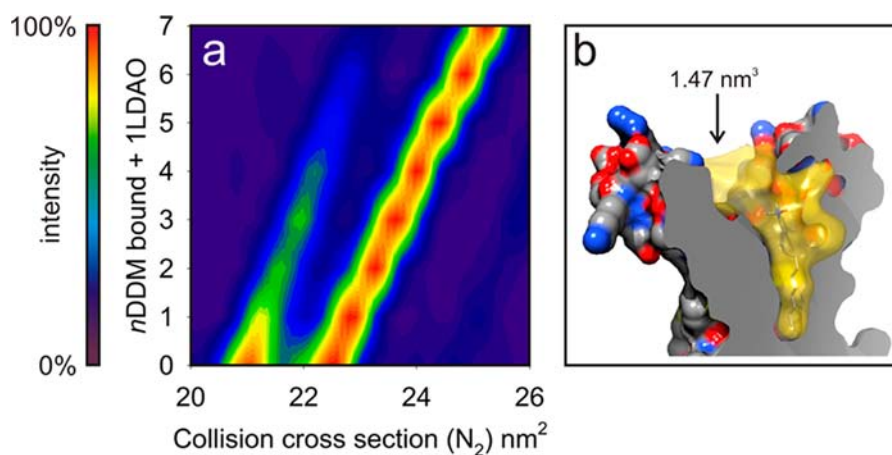


Figure 5. (a) ATD converted to Ω for the $[\text{PagP}:n\text{DDM}:1\text{LDAO}]^{6+}$ assemblies. (b) Lipid-binding cleft of PagP taken from the coordinates 1THQ with the AB loop reconstruction. PagP is shown with the view oriented from the E and F β -strands and the protein clipped to reveal the internal lipid-binding cavity and outer vestibule. Bound LDAO (shown) occupies a space of approximately 0.5 nm^3 based on the calculated partial molar volume of this detergent.²² The total volume of the lipid-binding cleft (yellow) is 1.47 nm^3 . The cavity volume was obtained using the 3 V cavity volume calculator with interior and exterior probe radii of 1.4 and 10 Å, respectively.²⁶ The lipid-binding cavity of PagP along with the protein is represented using the UCSF Chimera package from the Computer Graphics Laboratory, University of California, San Francisco.²⁷ Drift times were obtained on a Waters second generation Synapt HDMS in nitrogen.

were extracted for the collapsed and native-like conformations, respectively, for the DDM-free LDAO-bound protein, in line with values for the apo protein. This indicates that the gas-phase compaction of PagP does not involve the complete collapse of its lipid-binding cleft. The total volume of the lipid binding cleft of PagP is 1.47 nm^3 and bound LDAO would occupy a space of $\sim 0.5 \text{ nm}^3$ based on the calculated partial molar volume of this detergent (Figure 5b).²² Thus, only partial collapse of this cleft in the LDAO-bound form of the protein is feasible. We suggest therefore that the collapse of PagP is likely to be global with a significant contribution from the highly dynamic AB loop (Figure S4). Interestingly, the relative population of native-like conformations of PagP is increased in the LDAO-bound form of the protein (compare Figures 2 and 5a). Thus, while LDAO does not prevent the collapse of PagP entirely, the compaction of this protein is partially ameliorated by the presence of LDAO in the lipid-binding cavity.

CONCLUSION

Overall, in this study, we have shown that detergents directly affect the conformation of proteins in the gas-phase and that the preservation of native-like PagP depends on the presence of DDM. To obtain mechanistic insight into this process we have used MSMS-IMS to interrogate a range of different product ions obtained from a defined population of protein and detergent molecules. These experiments reveal a relationship between the extent of detergent release and the survival of native-like conformations in the gas-phase. This indicates that the process of releasing bound detergent in the gas-phase is central to the survival of the native-like conformations of PagP and the preservation of these species from conformational collapse.

Unlike previous gas-phase characterizations of membrane proteins, which typically employ high-energy conditions to promote dissociation of detergent micelles, these experiments have been performed at significantly lower energy to maintain

the protein-detergent interactions. Under these conditions, we propose that detergent release competes with conformational collapse for the available internal energy in the ions. The release of detergent decreases the energy available to the remaining assembly to overcome the barrier for conformational change. Further collisional heating of the assembly increases the internal energy of the ion and competition for this energy resumes. Ultimately, however, with depletion of detergent, structural collapse becomes the dominant pathway. Considerable parallels can be drawn between this study and the stabilizing influence of salt additives on soluble protein complexes in the gas-phase.^{23,24} Indeed the stabilizing action of bound anions is also thought to act via the release of these additives in the gas-phase.²⁵ The release of small molecules may therefore represent a general mechanism by which proteins and their complexes are stabilized in the gas phase. This study gives direct evidence that these phenomena can be exploited to improve the gas-phase characterization of membrane proteins.

■ ASSOCIATED CONTENT

📄 Supporting Information

Figure (S1) far UV CD spectrum of PagP along with gel-shift assay, (S2) linear fits for TWIMS calibration, (S3) isotropic growth of DDM clusters, and (S4) dynamic AB loop and lipid binding cleft of PagP; note discussing the population differences between Figure 2 and Figure 4b. This material is available free of charge via the Internet at <http://pubs.acs.org>

■ AUTHOR INFORMATION

Corresponding Author

carol.robinson@chem.ox.ac.uk

Notes

The authors declare no competing financial interest.

■ ACKNOWLEDGMENTS

The authors would like to thank Prof. Russell Bishop and Dr. Arthur Laganowsky for the kind gift of pETCrcAHΔS and modeling of the A/B loop of PagP, respectively. A.J.B. is a Waters Research Fellow, and C.V.R. is a Royal Society Professor funded by an ERC advanced fellowship.

■ REFERENCES

- (1) Barrera, N. P.; Di Bartolo, N.; Booth, P. J.; Robinson, C. V. *Science* **2008**, *321*, 243.
- (2) Barrera, N. P.; Isaacson, S. C.; Zhou, M.; Bavro, V. N.; Welch, A.; Schaedler, T. A.; Seeger, M. A.; Miguel, R. N.; Korkhov, V. M.; van Veen, H. W.; Venter, H.; Walmsley, A. R.; Tate, C. G.; Robinson, C. V. *Nat. Methods* **2009**, *6*, 585.
- (3) Zhou, M.; Morgner, N.; Barrera, N. P.; Politis, A.; Isaacson, S. C.; Matak-Vinkovic, D.; Murata, T.; Bernal, R. A.; Stock, D.; Robinson, C. V. *Science* **2011**, *334*, 380.
- (4) Wang, S. C.; Politis, A.; Di Bartolo, N.; Bavro, V. N.; Tucker, S. J.; Booth, P. J.; Barrera, N. P.; Robinson, C. V. *J. Am. Chem. Soc.* **2010**, *132*, 15468.
- (5) Borysik, A. J.; Robinson, C. V. *Langmuir* **2012**, *28*, 7160.
- (6) Borysik, A. J.; Robinson, C. V. *Phys. Chem. Chem. Phys.* **2012**, *14*, 14439.
- (7) Khan, M. A.; Neale, C.; Michaux, C.; Pomes, R.; Prive, G. G.; Woody, R. W.; Bishop, R. E. *Biochemistry-Us* **2007**, *46*, 4565.
- (8) Gupta, N.; Rathi, P.; Gupta, R. *Anal. Biochem.* **2002**, *311*, 98.
- (9) Bishop, R. E.; Gibbons, H. S.; Guina, T.; Trent, M. S.; Miller, S. I.; Raetz, C. R. H. *Embo J* **2000**, *19*, 5071.
- (10) Hernandez, H.; Robinson, C. V. *Nat. Protoc.* **2007**, *2*, 715.

- (11) Ruotolo, B. T.; Benesch, J. L.; Sandercock, A. M.; Hyung, S. J.; Robinson, C. V. *Nat. Protoc.* **2008**, *3*, 1139.
- (12) Bush, M. F.; Hall, Z.; Giles, K.; Hoyes, J.; Robinson, C. V.; Ruotolo, B. T. *Anal. Chem.* **2010**, *82*, 9557.
- (13) Guex, N.; Peitsch, M. C. *Electrophoresis* **1997**, *18*, 2714.
- (14) Qian, B.; Raman, S.; Das, R.; Bradley, P.; McCoy, A. J.; Read, R. J.; Baker, D. *Nature* **2007**, *450*, 259.
- (15) Mackerell, A. D., Jr.; Feig, M.; Brooks, C. L., 3rd. *J. Comput. Chem.* **2004**, *25*, 1400.
- (16) Giles, K.; Pringle, S. D.; Worthington, K. R.; Little, D.; Wildgoose, J. L.; Bateman, R. H. *Rapid Commun. Mass Spectrom.* **2004**, *18*, 2401.
- (17) Hwang, P. M.; Choy, W. Y.; Lo, E. I.; Chen, L.; Forman-Kay, J. D.; Raetz, C. R.; Prive, G. G.; Bishop, R. E.; Kay, L. E. *Proc. Natl. Acad. Sci. U.S.A.* **2002**, *99*, 13560.
- (18) Benesch, J. L.; Ruotolo, B. T. *Curr. Opin. Struct. Biol.* **2011**, *21*, 641.
- (19) Ahn, V. E.; Lo, E. I.; Engel, C. K.; Chen, L.; Hwang, P. M.; Kay, L. E.; Bishop, R. E.; Prive, G. G. *EMBO J.* **2004**, *23*, 2931.
- (20) Pagel, K.; Natan, E.; Hall, Z.; Fersht, A. R.; Robinson, C. V. *Angew. Chem., Int. Ed.* **2012**, *52*, 361.
- (21) Hwang, P. M.; Bishop, R. E.; Kay, L. E. *Proc. Natl. Acad. Sci. U.S.A.* **2004**, *101*, 9618.
- (22) Yalkowsky, S. H.; Zograf, G. *J. Pharm. Sci.* **1972**, *61*, 793.
- (23) Freeke, J.; Robinson, C. V.; Ruotolo, B. T. *Int. J. Mass Spectrom.* **2010**, *298*, 91.
- (24) Freeke, J.; Bush, M. F.; Robinson, C. V.; Ruotolo, B. T. *Chem. Phys. Lett.* **2012**, *524*, 1.
- (25) Han, L.; Hyung, S. J.; Mayers, J. J.; Ruotolo, B. T. *J. Am. Chem. Soc.* **2011**, *133*, 11358.
- (26) Voss, N. R.; Gerstein, M. *Nucleic Acids Res.* **2010**, *38*, W555.
- (27) Pettersen, E. F.; Goddard, T. D.; Huang, C. C.; Couch, G. S.; Greenblatt, D. M.; Meng, E. C.; Ferrin, T. E. *J. Comput. Chem.* **2004**, *25*, 1605.